Fuel Processing Technology 265 (2024) 108144

Contents lists available at ScienceDirect

Fuel Processing Technology

journal homepage: www.elsevier.com/locate/fuproc

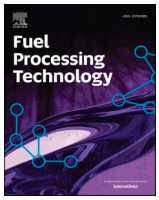

Impact of fuel and lubricant oil on particulate emissions in direct injection spark ignition engines: A comparative study of methane and hydrogen

Barbara Apicella [a], Francesco Catapano [a], Silvana Di Iorio [a], Agnese Magno [a], Carmela Russo [a,*], Paolo Sementa [a], Antonio Tregrossi [a], Bianca Maria Vaglieco [a]

[a] Institute of Science and Technology for Sustainable Energy and Mobility (STEMS) - CNR, Napoli, Italy

ARTICLE INFO

Keywords:
Particulate matter emission
Methane
Hydrogen
PAH
Spark ignition engine

ABSTRACT

Internal combustion engines play a critical role in the global transportation system and the use of alternative fuels, such as methane and hydrogen, offers a promising way for ensuring their sustainability in the future. The best way to exploit the gaseous fuels properties is through the direct injection that allows to enhance the efficiency and to prevent backfire issues. On the other hand, this injection strategy causes a high interaction of the lubricant oil in the combustion process and hence high level of particle emissions despite the low/zero carbon content in the fuels. An experimental study was conducted on a spark-ignition engine powered by directly injected methane. This study involved both physical and chemical characterization of emissions, with the aim of providing an in-depth analysis of the hazardous pollutants emitted. Additionally, it sought to identify their origins, whether from the fuel or lubricating oil. Experimental results show that a higher concentration of particles is produced at higher engine speed. In this condition, which has a more significant environmental impact, a comparison between methane and hydrogen-fueled engine operating under similar conditions was performed, revealing that hydrogen engine produces more particles with a smaller size.

1. Introduction

The need to pursuit a sustainable mobility has prompted to decrease the share of internal combustion engines (ICEs) based vehicles in favor of hybrid and electric technologies [1]. However, petrol cars still maintain a lead position in the European market [2] thus representing a relevant contributor of pollutant emissions, in particular the particles, in the urban area. It is well known in literature that the combustion process in ICEs produces soot particles in the highly fuel rich regions [3]. This soot tend to absorbs high molecular weight hydrocarbons from the oil and fuel and sulfur as sulfate during the expansion and exhaust strokes thus leading to the formation of particles [4].

Growing concern on atmospheric aerosol particles has accrued in the last years due to their adverse effects on human health and climate change [5]. Particle emissions are the main responsible of respiratory diseases and other health problems. The toxicity of the particles for the human being increases for the smaller ones since they can penetrate deeper in the respiratory system [6,7]. Moreover, the black carbon – soot - that is released from the burning of fossil fuel affects the Earth's temperature and climate by altering the radiative properties of the atmosphere [8].

In the last years, the carbon atoms present in the fuels have been recognized as the main source of particle emissions [9,10].

In the expectation of a complete electrification of the transport sector, made necessary by the ambitious goal of zero carbon dioxide (CO_2) emissions imposed by the European Union [1], low/zero carbon fuels represent a crucial bridging solution for the ICEs based transportation. Among the various alternative fuels, the liquid ones are recommended since they have high energy density, are easy to transport, distribute and store [11]. Alcohol fuels, methanol and ethanol, are particularly suitable for spark ignition engines thanks to their properties similar to those of gasoline [12]. *E*-fuels also have gained significant attention as a potential solution to reduce the carbon footprint associated with traditional fossil fuels. However, their sustainability depends on how hydrogen and electricity are produced [13]. Gaseous fuels, such as methane and hydrogen, also represent a valid solution to pursue the greenhouse gas reduction targets [14,15].

The advent of methane and hydrogen has led to the reduction of the particles produced by the fuel combustion but, on the other hand, the lubricant oil derived particles have carried more weight [16].

* Corresponding author at: Institute of Science and Technology for Sustainable Energy and Mobility (STEMS), Via G. Marconi 4, 80125 Naples, Italy.
E-mail address: Carmela.russo@stems.cnr.it (C. Russo).

https://doi.org/10.1016/j.fuproc.2024.108144
Received 23 April 2024; Received in revised form 18 September 2024; Accepted 10 October 2024
Available online 17 October 2024

Lubricant plays a crucial role in ensuring a smooth, efficient, and reliable operation of the engine. It forms a thin film on the moving parts that reduces the friction between the surfaces. Lubricant oil helps to remove byproducts like soot and sludge that can accumulate within the engine and to dissipate the heat from the hottest part of the engine. Moreover, it guarantees sealing gap thus preventing combustion gases from leaking past the piston rings and into the crankcase [17]. However, these functions cause oil consumption through different ways. Oil can, in fact, flows past the piston and valve guides into the combustion chamber or it can entrain in the cylinder through evaporation and blow-by [18].

Some studies have highlighted that the particle emissions can be influenced by lubricating engine oil properties and formulation [19–21] pointing out also that the health effects of exhaust particles may differ if they are lubricating oil or fuel derived owed to their chemical composition that affects their toxicity [22]. Therefore, to evaluate the impact of using a specific fuel, it is essential to consider all potential sources that could contribute to the emission of hazardous substances.

Accordingly, the shift towards low carbon footprint fuels, particularly those of gaseous type, has pointed out the need to understand how lubricant oil interacts with these fuels and influence the particle formation [23,24].

Singh et al. [25] observed that in compressed natural gas (CNG) engines, lubricant oil contributes significantly to the exhaust particle emissions since they do not provide for diesel particulate filter that can remove the inorganic fraction of particulate consisting of soot and trace metals and the three way catalytic converter just oxidizes the organic part of particulate.

However, the impact of lubricant oil on the particles emitted by gas fueled engines is still not clearly understood as also observed by Lahde et al. [26]. To fill this knowledge gap, they carried out an experimental activity consisting in the measurement of the particles emitted by a CNG fueled vehicle over worldwide light duty test cycles with three different oils. They concluded that a high ash, high volatility lubricant alters the solid particle number population in both >10 nm and > 23 nm size range revealing the importance of the lubricant quality.

The impact of lubricating oil on the particle emissions is even more important when hydrogen is used since it should not emit carbon-based emissions due to its chemical structure. Thawko et al. [27] investigated the particle emissions from a direct injection (DI) spark ignition (SI) engine with high compression-ratio fed with hydrogen, hydrogen-rich reformate, and methane. They observed that at specific operating conditions, the lower flame quenching distance of the hydrogen enhances the lubricant evaporation and consequently the particle formation leading to higher particle emissions with respect to methane.

It is worth underlining that the injection strategy also plays a significant role in the particle formation. Thawko et al. [28] performed an experimental comparison between port fuel injection (PFI) and DI of a reformate on the same engine highlighting the mechanisms responsible of higher particle formation with DI that are the high momentum jet - lubricated wall interaction, and the lubricant vapor entrainment into the gaseous fuel jet. In another study, Thawko et al. [29] observed high particle emissions when hydrogen is injected directly in the cylinder due to the greater involvement of lubricant oil in the combustion process. Therefore, they revealed a new challenge for hydrogen use in propulsion systems and pointing out the necessity to improve the knowledge on this topic to develop new methods of particle mitigation for hydrogen combustion.

Although it is known in literature the presence of particle emissions at exhaust of SI engines fueled with gaseous fuels because of the contribution of lubricant oil, there is a lack of knowledge about the mechanisms responsible of their formation. To this purpose, an extensive research was carried out by the authors consisting in the physical and chemical characterization of the species emitted from a SI engine fueled with direct injected hydrogen in to better understand the phenomena involved in the oil transformation and, hence, responsible for particle formation [30,31].

This research study was extended to another gaseous fuel at low carbon content, the methane. The present work, in fact, characterizes the particles emitted by a single cylinder, 250 cm^3, SI engine fueled with methane in DI mode. Experiments were carried out at two engine test points reflecting typical urban driving conditions. The originality of the study with respect to the existing literature consists in the simultaneous application of different techniques for both the physical and chemical characterization of the particles. Particle number and size were measured through on-line measurements on the diluted exhaust. Spectroscopic and chemical techniques were, instead, implemented off-line on the condensed exhaust and on the particles collected on a filter. Insights on the carbon source of the pollutants are given. Finally, carbon particle emissions from methane-fueled engine are discussed comparing these data with those from our previous studies [30,31] on hydrogen-powered engines under similar conditions. This comparison aims to evaluate particle emissions between the cleanest fossil fuel and one of the most promising carbon-free fuel.

2. Experimental apparatus and methods

2.1. Test engine

Experiments were carried out on a single-cylinder SI engine loaded by an electrical dynamometer. It is based on a series production engine featured with a DI system consisting of a side-mounted, six-hole injector for liquid fuels located between the intake valves. More details about the technical specification of the engine are given in Table 1.

Due to the lack of any commercial injectors for the DI of gaseous fuels, a system was developed in house by employing an air strata injector typically used for the simultaneous injection of air and gasoline and it was set in the cylinder head through a specifically designed adaptor [32]. Methane and hydrogen were supplied from pressurized 200 bar bottles. The gas pressure was reduced to 6 bar by a regulator and then supplied to the cylinder. A flashback arrestor together with a pneumatic-actuated valve were placed in the hydrogen supply line to avoid the hazard of the flame propagation towards the cylinder in case of backfire.

A dedicated engine timing unit (ETU) allowed to control ignition and injection parameters.

An oxygen sensor (LSU 4.9 Bosch) was installed in the exhaust manifold and connected to a lambda meter (LA4, ETAS) to monitor real time the operating excess air ratio (λ).

A piezoelectric pressure transducer (AVL GH12D) mounted on the cylinder head along with a crank angle encoder allowed to measure the crank angle resolved indicated data.

The oil used for the engine lubrication was a synthetic blend with an SAE 10 W-40 viscosity grade whose main properties are listed in Table 2.

2.2. Experimental layout for particles characterization

A scheme of the experimental setup for the particle investigation is shown in Fig. 1.

Particle emissions were characterized from a physical point of view

Table 1
Engine specifications.

Engine	Spark Ignition
Number of Cylinders	1
Bore [mm]	72
Stroke [mm]	60
Displacement [cm^3]	244.3
Compression Ratio	11.5:1
Max. Power [kW]	16 @ 8000 rpm
Max. Torque [Nm]	20 @ 5500 rpm
Intake	Naturally Aspirated
Injection system	DI Prototype

Table 2
Lubricant oil properties.

Properties	
Viscosity	10 W-40
Density @ 20 °C	0.870 kg/l
Viscosity @ 40 °C	101.7 mm^2/s
Viscosity @ 100 °C	14.5 mm^2/s
Viscosity index	151
Pour point	−35.0 °C
TBN	10.1 mg KOH/g
Flash point	228 °C

through on-line measurements of diluted exhaust during the engine running. The TSI Engine Exhaust Particle Sizer (EEPS) 3090 allowed to measure the temporal particle concentration as well as the particle number-size distribution in the range 5.6–560 nm at 10 Hz frequency. EEPS specifications and detailed working principle can be referred in the instrument manual [33]. Before entering the EEPS, the exhaust gas was sampled through a 150 °C heated probe to prevent water condensation and then it was diluted at a ratio of 1:9 by a single diluter (SD).

The condensed exhaust and the particles gathered at the tailpipe were analyzed in detail through an off-line chemical characterization.

Cleaning the sampling line, extracting condensed water liquid-to-liquid, and separating the dichloromethane (DCM)-soluble portion of the sample collected on the filter all contributed to the recovery of the soluble organic fraction (SOF), whereas soot represents the DCM-insoluble portion. More details on the sampling approach and sample treatments are reported in [30,31].

The composition of SOF samples was characterized by gas chromatography mass spectrometry (GC–MS) using an AGILENT GC 6890 - MSD 5975C. More details are reported on GC–MS measurements are reported in [30,31]. Using an HP 8453 Diode Array spectrophotometer, the UV–visible spectra of SOF samples dissolved in DCM were acquired in a 1-cm path length quartz cuvette. SOF fluorescence spectra were measured on a HORIBA Scientific FluoroMax-Plus TCSPC spectrofluorometer. More details on the acquisition of fluorescence spectra are reported in [34]. Molecular Weight (MW) distributions of SOF and soot samples were measured by size exclusion chromatography (SEC) by elution with *N*-methyl pyrrolidone (NMP) on a High Pressure Liquid Chromatography (HPLC) system HP1050 series measuring the absorbance value of eluting species at 350 nm with an UV–Visible diode array detector. For the purpose of determining mass in the range of 100–2E4 u and 2E3–4E8 u, respectively, the MW distributions of SOF samples were measured on two distinct columns: a highly cross-linked "individual-pore" column (Polymer Laboratories, Ltd., U.K.; particle size of 5 μm diameter and a pore dimension of 50 nm) and a Jordi Gel DVB Column. On both columns the operative conditions were optimized for species/particles separation. In the first case the injection volume was 100 μl and the analyses were performed at 70 °C with a flow rate of 0.5 ml/min, while in the second case measurements were conducted at ambient temperature with an injection volume of 10 μl and a flow rate of 0.8 ml/min. SEC chromatogram of soot was acquired only on the Jordi GEL DVB column. The MW calibration of both columns was obtained using standard species with known MW and carbon particles with known sizes [35].

2.3. Operating conditions

In the first part of the study, the characterization of the particle emissions was carried out by fueling the engine with methane. All measurements were taken during steady state speed and load conditions. In particular, experiments were carried out at two operating conditions characteristic of urban driving cycles characterized by the engine speeds of 2000 and 3000 rpm and 6 bar of indicated mean effective pressure (imep). Then, a comparison of the particles emitted by methane with respect to hydrogen was performed at the test point 3000 rpm - 6 bar.

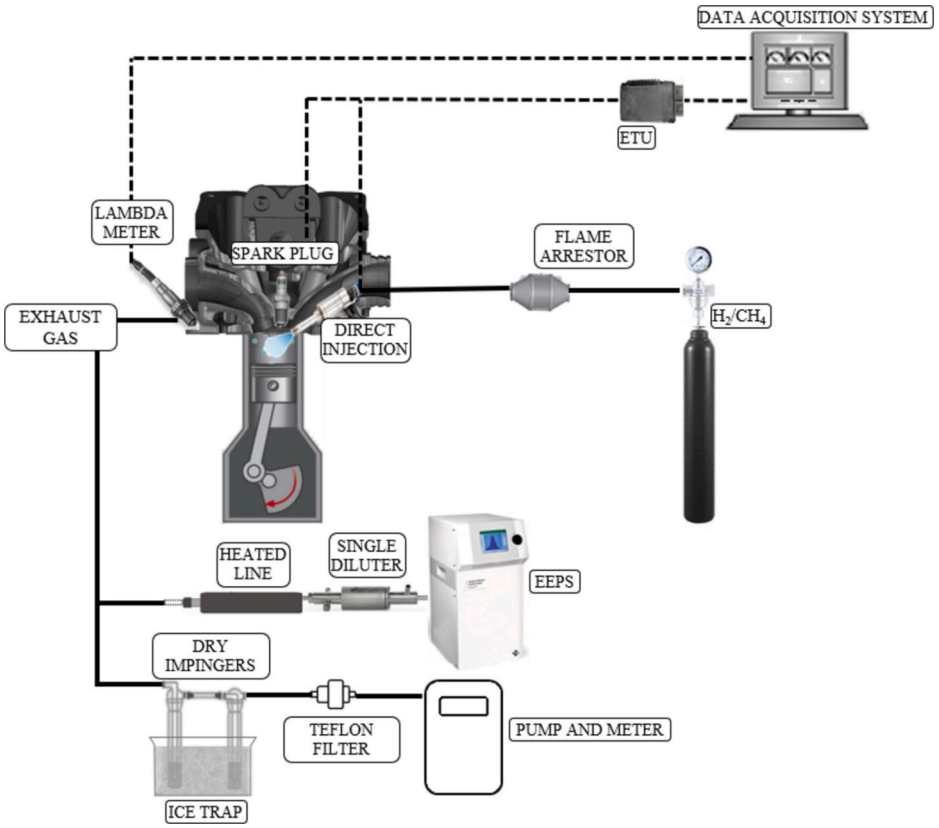

Fig. 1. Experimental layout.

The engine parameters of the tested conditions are summarized in Table 3. The start of injection (SOI) and start of spark (SOS) were chosen to guarantee a stable combustion as also proved by the coefficient of variation (COV) of imep that assumed values below 2 %. The duration of injection (DOI) was modified to operate in lean conditions thus preventing the nitrogen oxides (NO_x) emissions. Tests with methane were realized at throttled conditions and, because of its narrow flammability limits, the maximum λ value reachable that allowed a stable combustion was 1.2. For hydrogen, wide open throttle (WOT) operation was realized. Thanks to its favorable properties, as wide flammability range, the combustion was stable at higher λ values, and it was chosen to work at λ 1.6.

Condensed exhaust samples were collected during engine running at fixed operating condition. Three samples were acquired for each test point. The total uncertainty of the chemical and spectroscopic results, taking into account the sampling, the sample treatment and preparation, and the analytical measurements, was around 15 %. For each condition, particle size distributions (PSDs) were detected 5 times for a duration of 2 min. The variability among the different acquisitions was below 5 %.

3. Experimental results

The discussion of the experimental results is organized as follows. The first part is focused on the particles emitted by methane. They were physically and chemically characterized at two operating conditions to understand the involvement of lubricant oil in the combustion process and, consequently, on the particle formation. The second part, instead, presents a comparison between methane and hydrogen. Previous studies by the Authors [30,31] have detailed investigated the particle emissions due to the lube oil for hydrogen fueling and the impact of the operating condition. It was found out that in the condition at 2000 rpm and 6 bar of imep, the particles emitted were within the limit values of the spectrometer due to low signal to noise ratio. Since at this test point the conventional techniques did not provide relevant information on the particle emissions, for a more comprehensive comparison between methane and hydrogen the test point at 3000 rpm – 6 bar, characterized by the highest particle concentration, was selected.

3.1. Physical particle characterization for methane fueling

Fig. 2 shows the contour plot representing the particle number and diameter over 2 min of acquisition for methane at both investigated conditions.

At 2000 rpm, the measured particle concentration is quite low reaching values slightly higher than the lower limit of the spectrometer. It can be observed a peak concentration of about 10^5 #/cm^3 centered at 10 nm. The concentration is one order of magnitude lower in the size range 20–60 nm.

Higher particle concentration is measured at 3000 rpm. At higher engine speed, particles range between 10 and 100 nm and they reach a peak concentration of order of magnitude around 10^6 #/cm^3. When methane fuel is burnt, the source of particle emissions could be the carbon atoms present in the fuel even if the major contribution is given by the lubricant oil. Oil consumption due to evaporation and blow-by entrainment increases with the engine speed [36] thus explaining the larger number of particles emitted at 3000 rpm. As also observed by Amirante et al. [37], lubricant oil increases the number of the smaller particles. Nevertheless, when the involvement of lubricant is consistent,

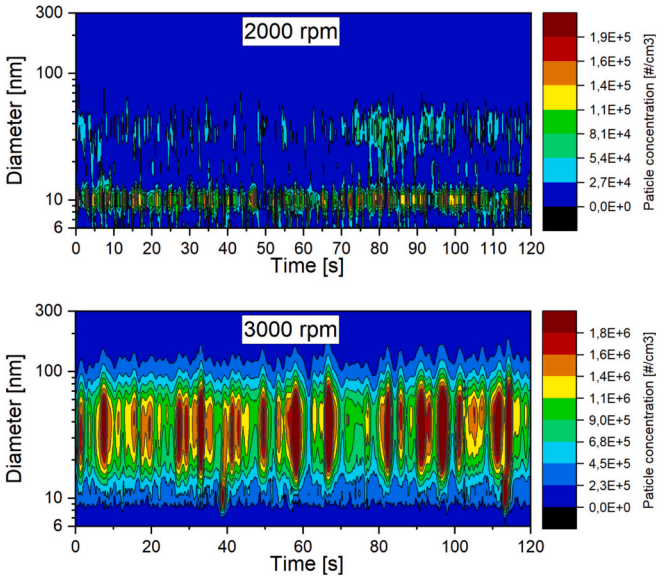

Fig. 2. Time-resolved particle concentration and size distributions for methane at 2000 and 3000 rpm.

also particles larger than 50 nm appear in appreciable quantities.

An interesting result arising from Fig. 2 consists in the temporal fluctuation of the particle concentration. Although the test was carried out at fixed operating condition, the particle concentration is not uniform throughout the test, but it exhibits temporal oscillations. This behavior was also observed by the authors for hydrogen fuel [31] identifying the cause in the lubricant oil since hydrogen does not contain carbon atoms that can be responsible of the particle formation. This fluctuation is explained by the potential periodic oil accumulation on the cylinder surfaces that, reached by the flame front, participate to the combustion process and, hence, to the mechanisms of particle formation.

To better investigate the particles emitted by methane combustion, the number concentration (N), classified in the particles lower ($N < 23$ nm) and larger ($N > 23$ nm) than 23 nm, was calculated at both investigated conditions as shown in Fig. 3. At 2000 rpm (inner circle), the particle number concentration reaches low values, and it is almost equally distributed between the sub 23 nm particles (51 % of total) and the larger of 23 nm ones (49 %). At 3000 rpm, instead, the particle number concentration is higher, and it consists of 35 % of $N < 23$ nm particles and for the 65 % of the $N > 23$ nm particles. The increase of the particle number with the engine speed can be ascribed to the larger oil consumption as well documented in literature. Incomplete combustion and pyrolysis of high molecular weight hydrocarbons present in the oil result in the formation of nuclei particles that tend to agglomerate into accumulation particles.

3.2. Chemical particle characterization for methane fueling

The SOF samples were analyzed by GC–MS to get insights into their composition. The GC–MS chromatograms obtained along with that of the lubricating oil are reported in Fig. 4.

Differently from what observed for the SOF samples derived from

Table 3
Operating conditions.

Fuel	Engine speed [rpm]	Throttle opening [%]	DOI [cad]	SOI [cad BTDC]	SOS [cad BTDC]	λ [−]	imep [bar]	COV imep [%]
Methane	2000	8	175	305	22.5	1.2	6.0	1.03
	3000	4	240	315	15.0	1.2	6.0	0.96
Hydrogen	3000	95	245	352	10.0	1.60	6.0	1.65

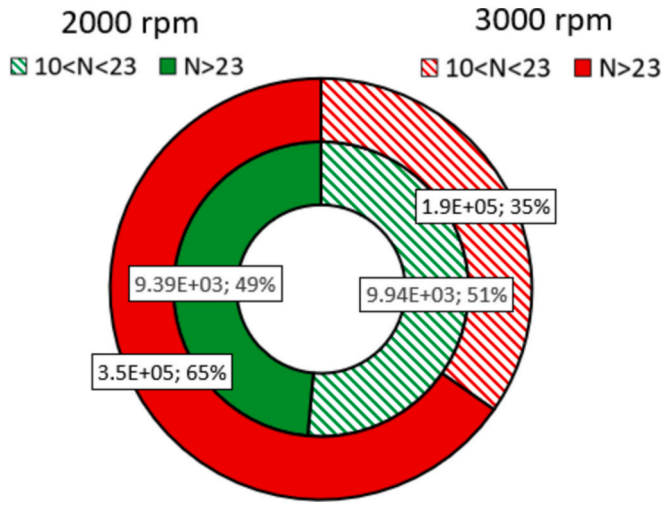

Fig. 3. Particle number concentration, classified in $N < 23$ and $N > 23$ nm, emitted by methane at 2000 (inner circle) and 3000 rpm (outer circle).

tests on hydrogen-fueled engines [31], the SOF chromatograms do not resemble totally to those of the lubricating oil, suggesting that the fuel and the oil contribute to particle formation. The SOF at 3000 and the oil sample are characterized by a similar bump from 40 to 55 min. In both cases a sequence of alkanes was detected by ion extraction in this retention time range. The concentration of the species was very low in the 2000 rpm sample and no peak presents a satisfying match quality when matched with mass spectra library. The 3000 rpm sample presents more intense peaks and aromatic species represent the 5 wt% of this sample.

It is worth underlining that just a small fraction of the SOF samples was detected and identified by GC–MS.

To obtain a comprehensive understanding of the types of particles and molecular species emitted from methane-fueled engines, SOF samples were subjected to a variety of chemical and spectroscopic analyses. Fig. 5, reporting the MW distributions measured on the not-mixed column, provides an overview of the lighter species and smaller particles composing SOF. Both distribution functions exhibit signals at similar MW values, presenting a broad peak in the region extending between 200 and 2000 u and a sharper peak in the region around 10^4 u. Assuming spherical particles and densities in the 1.2–1.8 g/cm^3 range, the first area corresponds to molecules with a hydrodynamic diameter around 1–2 nm and the second peak refers to particles of about 3–5 nm.

Looking at the relative peak intensity ratio, the largest contribution of light molecular species in the 3000 rpm sample, is the sole notable variation between the samples. Comparing the SEC profiles normalized for the sampled volume (Fig. 5-panel A), it is possible to observe the very different signal intensity and, therefore, species concentration in the two conditions: species are more than twenty times more concentrated at the higher engine speed.

The SOF composition can be further elucidated through spectroscopic investigation. All the optical measurements acquired on the SOF samples are reported in Fig. 6. The UV–visible spectra of the SOF samples, normalized at 350 nm, are shown in Fig. 6 A. Despite varying the engine speed, they all seem to have relatively similar spectral characteristics. The absence of a fine structure typical of PAH molecules indicated that these species give a negligible contribute, confirming GC–MS data, and that larger aromatic species are present [34].

Fluorescence spectroscopy is more sensitive than UV–Visible spectroscopy in the identification of even subtle differences in highly-fluorescence species as PAHs. The emission spectrum of a PAH mixture usually presents signals in two main wavelength regions: the first one is located from 300 to 350 nm and is caused primarily by two- and three-ring PAHs; the second falls between 350 and 500 nm and is caused mostly by bigger PAHs (3–6 rings) [38]. As the number of rings constituting the molecules increases, the fluorescence can be excited with higher excitation wavelengths. The emission spectra obtained with an excitation wavelength of 250 nm (panel B) and of 350 nm (panel D) are reported in Fig. 6. It can be noticed that the spectrum obtained with a higher excitation energy presents the fine structure typical of small aromatic molecules. Overall, the spectral features of SOF samples are very similar, just a more intense tail at higher wavelengths can be noticed at 3000 rpm underlying the presence of PAHs with a high number of rings.

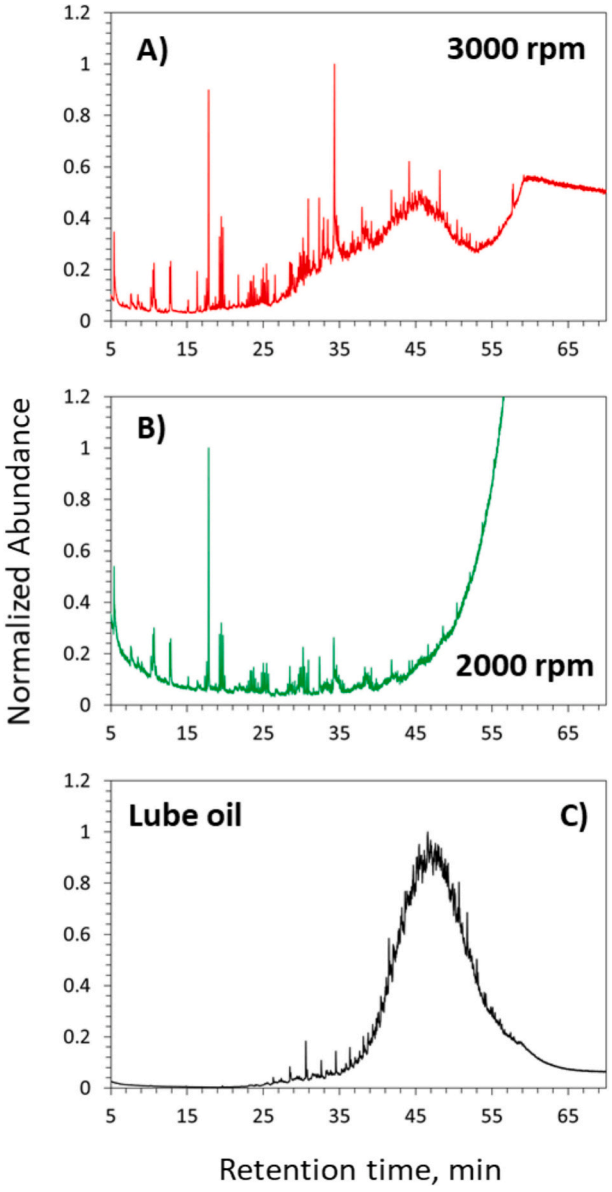

Fig. 4. GC–MS chromatograms of SOF of at 3000 rpm (A) and 2000 rpm (B) along with the lubricant oil chromatogram (C).

The analysis of the fluorescence spectrum of aromatic mixtures can give more quantitative information on PAH distribution looking at the synchronous fluorescence, where each peak can be attributed to a class of components [39,40]. As the ring number rises, the synchronous peak shifts at longer wavelengths. The synchronous spectra, reported in the panel C of Fig. 6, indicate that 3000 rpm sample present a higher contribution of species with 3–6 aromatic rings whereas the sample at 2000 rpm has a PAH distribution shifted at lower masses.

Soot, defined as the fraction not soluble in dichloromethane (DCM), was detected exclusively at 3000 rpm. SOF and soot samples were also

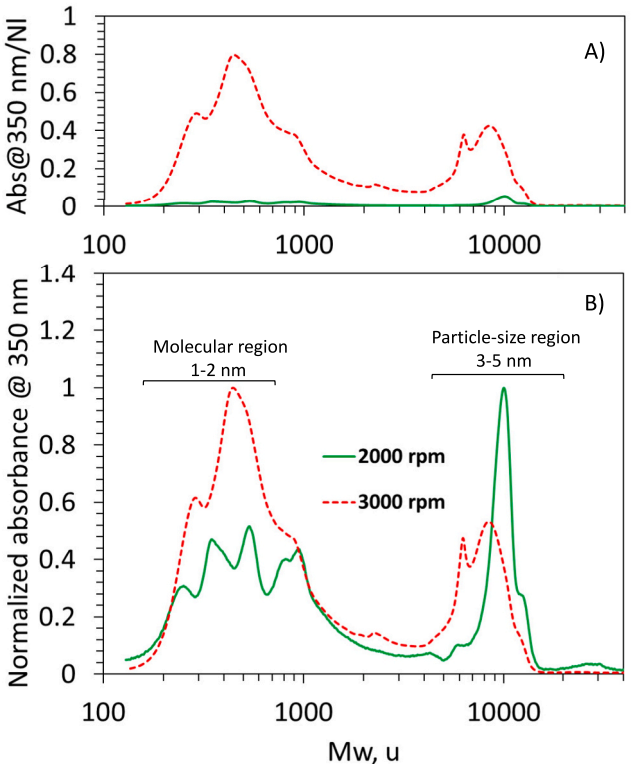

Fig. 5. MW distribution profiles A) normalized for the sampled volume and B) normalized on the peak maximum intensity of the SOF samples from SEC with not mixed column of 2000 and 3000 rpm samples, acquired with UV–Visible detector at 350 nm.

analyzed with a no porous column to better detect carbon nanoparticles and aggregates. In Fig. 7 the MW distributions of both SOF samples and of the soot sample only at 3000 rpm are reported along with the normalized PSDs measured by the EEPS. For a proper comparison between the on-line (EEPs) and offline (SEC) techniques used in this paper to track particle size, PSDs, measuring together soluble and insoluble particles, have to be contrasted with SOF and soot chromatograms. At 3000 rpm the MW distributions of soot and SOF are peaked at MW values corresponding to particles with a dimension of 2–10 nm. The soot at 3000 rpm presents an additional broad peak attributable to larger particles/aggregates with a mean size of 60 nm. The normalized PSD shows a main peak at size around 10 nm and a second minor peak at around 60 nm at 3000 rpm, as found by SEC analysis. Also, at 2000 rpm the online and offline distributions present two sharper peaks, the first one located at around 10 nm. For EEPS the second peak is located at around 40 nm while for SEC at lower size. This slight discrepancy could be due to the fact that these organic particles belonging to SOF can be highly sticky and in the aerosol they could present a larger size compared to when dissolved in a powerful solvent as NMP.

3.3. Comparison of particle emissions due to methane and hydrogen

As above explained, the particle emissions from ICEs can be ascribed to both the fuel and the lubricant oil and the latter can contribute differently to the particle formation depending on the fuel characteristics. In this section, the particles emitted by methane were compared to those of a carbon-free fuel, i.e., hydrogen, for which the particles measured at exhaust are produced exclusively by the lubricant oil. Fig. 8 displays a comparison in terms of number, size and mass of the particles emitted by methane and hydrogen at the test point characterized by the higher particle concentration (Fig. 2) that is 3000 rpm - 6 bar.

The histogram in the graph shows the percentage variation of the particles emitted by hydrogen with respect to methane in both dimensional ranges, $N < 23$ and $N > 23$ nm. The positive values are indicative of higher number of particles, especially those of smaller diameter, measured with hydrogen.

In Fig. 9 the MW distributions of particles emitted from methane and hydrogen fueled engine are contrasted both when contained in SOF (panel A) and in soot (panel B). According with the data reported in Fig. 8, the particles emitted by hydrogen are mainly featured by a size ranging from 2 to about 10 nm. In the methane case, particle sizes are peaked at 10 nm with also a presence of a minor peak at very large size (peak at about 60 nm).

The particle emission profiles of both fuels can be justified by their combustion behavior. As observed by the authors in their previous studies [41–43], hydrogen is characterized by higher heat release and a fast combustion with respect to methane. Higher heat release also results in increased temperature and pressure with the subsequent reduction in the flame quenching distance. As a consequence, the flame comes closer to the piston surface, then the high flame temperature of hydrogen combustion [15] enhanced lubricant evaporation on the cylinder surfaces that partially burns during combustion process thus leading to the soot precursor formation. Moreover, the shortened combustion duration, due to relatively faster fuel-air combustion kinetics, prevents the coagulation of particulate resulting in higher nucleation mode particles [44].

On the other hand, the PSD of methane is shifted towards larger diameter particles as proved by the geometrical mean diameter (GMD) that is 60 nm with respect to 39 nm measured for hydrogen. This trend can be ascribed to the lower flame temperature of the methane thus preventing the oxidation mechanisms of the particles and leading to larger diameter particle formation [45]. Despite the larger number for hydrogen fueling, the methane gives the major contribution to the particle mass as proved by the larger emission of particles larger than 70 nm.

4. Conclusions

This work sheds light on the particles emitted by a SI engine fueled with gaseous fuels, methane and hydrogen, injected in direct mode. The work was characterized by the innovative use of different and complementary techniques allowing simultaneously the physical and chemical characterization of the particles. The first part of the study was focused on the investigation of the particles emitted by methane fueled engine. A comparison was then made with hydrogen, a zero-carbon fuel, to provide valuable insights into the fuel-oil interaction in the mechanisms of particle formation. The major results can be summarized as follows:

- Particles emitted by methane combustion increase in number and size with the engine speed, a certain contribute of the oil was found at the higher engine speed.
- Hydrogen emits a higher number of smaller diameter particles. Methane combustion emits totally lower number of particles that are characterized by larger diameter thus impacting more on the mass.
- Although for methane fueling the particle emissions cannot be clearly attributed to the incomplete combustion of oil or fuel, it is clear that for hydrogen the lube oil has a more significant impact on the number of particles emitted.

Results arising from this study could be beneficial for the lubricating oil development and formulation considering the necessity to abate the exhaust emissions of particles from the vehicles. By addressing the lubricating oil issue, in fact, methane and even more hydrogen can live up to their full potential as clean and sustainable fuels for transportation. This is a crucial field of research due to the expected massive use in the transportation sector of low emission fuels as well as the need to limit the particle emissions in the congested urban area.

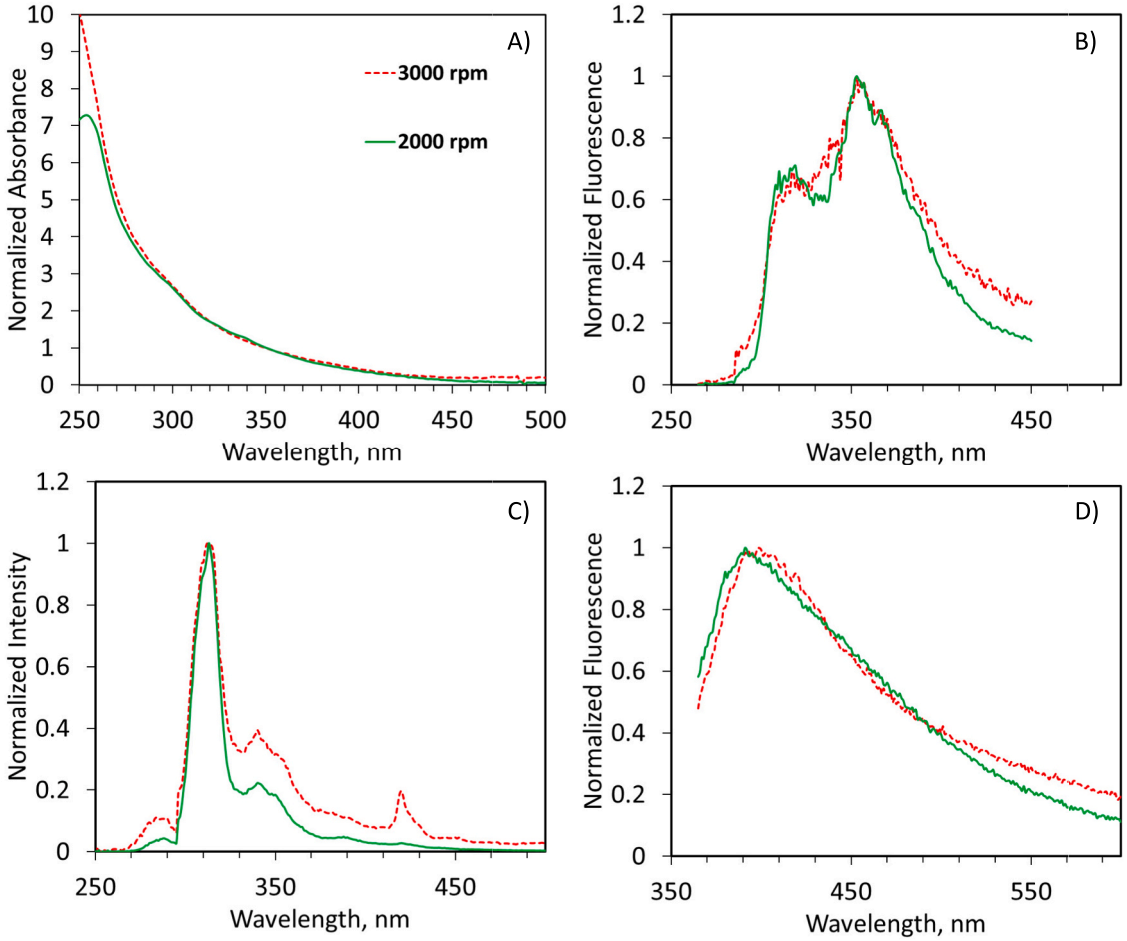

Fig. 6. Height normalized UV–Visible absorption spectra (A), height normalized emission spectra excited at 250 (B) and 350 (D) nm and height normalized synchronous fluorescence spectra (C) ($\Delta\lambda = 10$ nm) of SOF in DCM at 2000 and 3000 rpm.

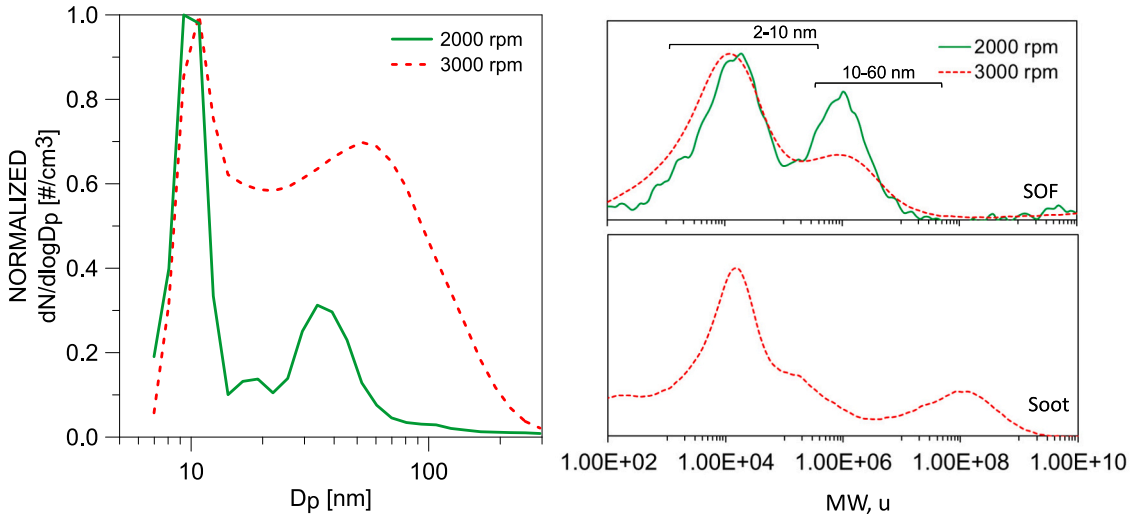

Fig. 7. Height normalized MW distribution profiles of the soot and SOF samples from SEC analysis for methane at 2000 and 3000 rpm and LL, acquired with UV–Visible detector at 350 nm compared with the normalized PSDs measured by EEPS.

CRediT authorship contribution statement

Barbara Apicella: Writing – original draft, Visualization, Methodology, Investigation, Data curation, Conceptualization. **Francesco Catapano:** Methodology, Investigation. **Silvana Di Iorio:** Writing – original draft, Visualization, Methodology, Investigation, Data curation, Conceptualization. **Agnese Magno:** Writing – original draft, Visualization, Methodology, Investigation, Data curation, Conceptualization. **Carmela Russo:** Writing – original draft, Visualization, Methodology, Investigation, Data curation, Conceptualization. **Paolo Sementa:**

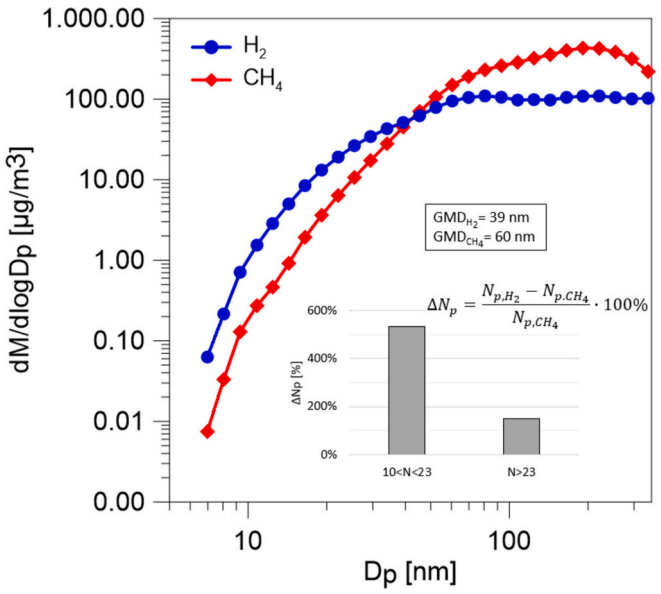

Fig. 8. Particle mass distribution and particle number variation for hydrogen and methane at 3000 rpm.

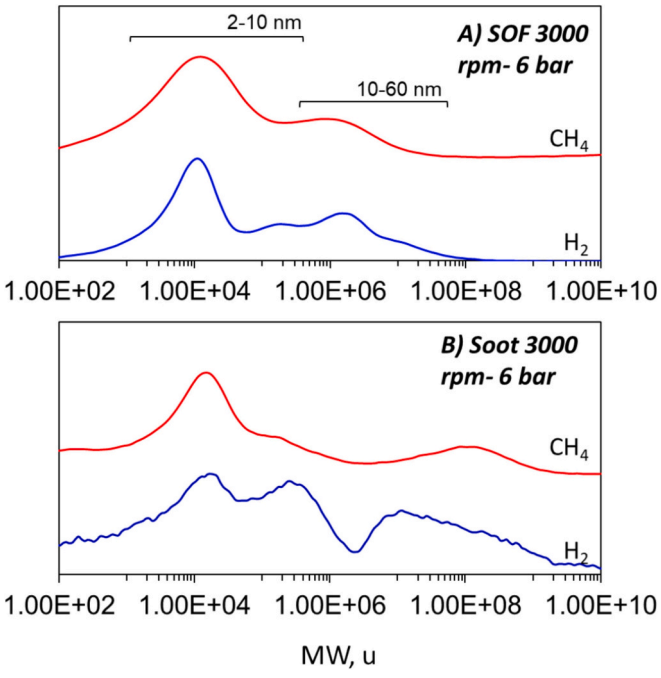

Fig. 9. MW distribution profiles of the soot (panel B) and SOF (panel A) samples from SEC analysis for methane and hydrogen at 3000 rpm acquired with UV–Visible detector at 350 nm.

Methodology, Investigation. **Antonio Tregrossi:** Methodology, Investigation. **Bianca Maria Vaglieco:** Writing – review & editing, Supervision.

Declaration of competing interest

The authors declare that they have no known competing financial interests or personal relationships that could have appeared to influence the work reported in this paper.

Data availability

Data will be made available on request.

Acknowledgments

This research has been partially supported by the European Union - NextGenerationEU - National Sustainable Mobility Center CN00000023, Italian Ministry of University and Research Decree n. 1033-17/06/2022, Spoke 12, CUP B43C22000440001.

Authors thank Carlo Rossi and Bruno Sgammato for the engine assessment and for the support in the experimental activity.

References

[1] 2050 Long-Term Strategy. https://climate.ec.europa.eu/eu-action/climate-strategies-targets/2050-long-term-strategy_en, 2024 (accessed March 27, 2023).
[2] ACEA. https://www.acea.auto/pc-registrations/new-car-registrations-12-1-in-january-2024-battery-electric-10-9-market-share/, 2024.
[3] P. Eastwood, Particulate Emissions from Vehicles, England, 2008, https://doi.org/10.1002/9780470986516.
[4] J.B. Heywood, Chapter 1 - Motor vehicle emissions control: past achievements, future prospects, in: E. Sher (Ed.), Handb. Air Pollut. From Intern. Combust. Engines, 1998, pp. 3–23, https://doi.org/10.1016/B978-0-12-639855-7.X5038-8.
[5] C.A. Pope, M. Ezzati, D.W. Dockery, Fine-particulate air pollution and life expectancy in the United States, N. Engl. J. Med. 360 (2009) 376–386, https://doi.org/10.1056/NEJMsa0805646.
[6] B. Giechaskiel, U. Manfredi, G. Martini, Engine exhaust solid sub-23 nm particles: I. Literature survey, SAE Int. J. Fuels Lubr. 7 (2014) 950–964, https://doi.org/10.4271/2014-01-2834, 2014-01-2834.
[7] B. Alföldy, B. Giechaskiel, W. Hofmann, Y. Drossinos, Size-distribution dependent lung deposition of diesel exhaust particles, J. Aerosol Sci. 40 (2009) 652–663, https://doi.org/10.1016/j.jaerosci.2009.04.009.
[8] Mark Z. Jacobson, Strong radiative heating due to the mixing state of black carbon in atmospheric aerosols, Nature 409 (2001) 695–697.
[9] Z. Li, J. Liu, Q. Ji, P. Sun, X. Wang, P. Xiang, Influence of hydrogen fraction and injection timing on in-cylinder combustion and emission characteristics of hydrogen-diesel dual-fuel engine, Fuel Process. Technol. 252 (2023) 107990, https://doi.org/10.1016/j.fuproc.2023.107990.
[10] E. Jiaqiang, X. Wanrong, M. Yinjie, T. Dongli, P. Qingguo, T. Yan, et al., Soot formation mechanism of modern automobile engines and methods of reducing soot emissions: a review, Fuel Process. Technol. 235 (2022) 107373, https://doi.org/10.1016/j.fuproc.2022.107373.
[11] T. Larsson, O. Stenlaas, A. Erlandsson, Future fuels for DISI engines: a review on oxygenated, in: Liquid Biofuels 2019, SAE Tech Pap, 15 Jan 2019, https://doi.org/10.4271/2019-01-0036.
[12] A.K. Agarwal, H. Karare, A. Dhar, Combustion, performance, emissions and particulate characterization of a methanol-gasoline blend (gasohol) fuelled medium duty spark ignition transportation engine, Fuel Process. Technol. 121 (2014) 16–24, https://doi.org/10.1016/j.fuproc.2013.12.014.
[13] S. Dell'Aversano, C. Villante, K. Gallucci, G. Vanga, A. Di Giuliano, E-Fuels: a comprehensive review of the most promising technological alternatives towards an energy transition, Energies 17 (2024) 1–43, https://doi.org/10.3390/en17163995.
[14] K. Nguyen Duc, V. Nguyen Duy, L. Hoang-Dinh, T. Nguyen Viet, T. Le-Anh, Performance and emission characteristics of a port fuel injected, spark ignition engine fueled by compressed natural gas, Sustain. Energy Technol. Assessm. 31 (2019) 383–389, https://doi.org/10.1016/j.seta.2018.12.018.
[15] D. Akal, S. Oztuna, M.K. Büyükakın, A review of hydrogen usage in internal combustion engines (gasoline-Lpg-diesel) from combustion performance aspect, Int. J. Hydrog. Energy 45 (2020) 35257–35268, https://doi.org/10.1016/j.ijhydene.2020.02.001.
[16] A.L. Miller, C.B. Stipe, M.C. Habjan, G.G. Ahlstrand, Role of lubrication oil in particulate emissions from a hydrogen-powered internal combustion engine, Environ. Sci. Technol. 41 (2007) 6828–6835, https://doi.org/10.1021/es070999r.
[17] H. Yi, J. Seo, Y.S. Yu, Y. Lim, S. Lee, J. Lee, et al., Effects of lubricant-fuel mixing on particle emissions in a single cylinder direct injection spark ignition engine, Sci. Rep. (2022) 12, https://doi.org/10.1038/s41598-021-03873-w.
[18] J.B. Heywood, Internal Combustion Engine Fundamentals 26, United States of America, 1988, https://doi.org/10.5860/choice.26-0943.
[19] L. Dong, G. Shu, X. Liang, Effect of lubricating oil on the particle size distribution and total number concentration in a diesel engine, Fuel Process. Technol. 109 (2013) 78–83, https://doi.org/10.1016/j.fuproc.2012.09.040.
[20] S. Brandenberger, M. Mohr, K. Grob, H.P. Neukom, Contribution of unburned lubricating oil and diesel fuel to particulate emission from passenger cars, Atmos. Environ. 39 (2005) 6985–6994, https://doi.org/10.1016/j.atmosenv.2005.07.042.
[21] V. Premnath, I. Khalek, P. Morgan, A. Michlberger, M. Sutton, P. Vincent, Effect of Lubricant Oil on Particle Emissions from a Gasoline Direct Injection Light-Duty Vehicle, SAE Tech Pap, 2018, pp. 1–5, 2018-01-1708, https://doi.org/10.4271/2018-01-1708.
[22] M.J. Kleeman, S.G. Riddle, M.A. Robert, C.A. Jakober, Lubricating oil and fuel Contributions to particulate matter emissions from light-duty gasoline and heavy-

duty diesel vehicles, Environ. Sci. Technol. 42 (2008) 235–242, https://doi.org/10.1021/es071054c.
[23] C.P. García, S. Orjuela Abril, J.P. León, Analysis of performance, emissions, and lubrication in a spark-ignition engine fueled with hydrogen gas mixtures, Heliyon (2022) 8, https://doi.org/10.1016/j.heliyon.2022.e11353.
[24] A.P. Singh, D. Kumar, A.K. Agarwal, Particulate characteristics of laser ignited hydrogen enriched compressed natural gas engine, Int. J. Hydrog. Energy 45 (2020) 18021–18031, https://doi.org/10.1016/j.ijhydene.2020.05.005.
[25] A.P. Singh, A. Pal, A.K. Agarwal, Comparative particulate characteristics of hydrogen, CNG, HCNG, gasoline and diesel fueled engines, Fuel 185 (2016) 491–499, https://doi.org/10.1016/j.fuel.2016.08.018.
[26] T. Lähde, B. Giechaskiel, G. Martini, K. Howard, J. Jones, S. Ubhi, Effect of lubricating oil characteristics on solid particle number and CO2 emissions of a Euro 6 light-duty compressed natural gas fuelled vehicle, Fuel (2022) 324, https://doi.org/10.1016/j.fuel.2022.124763.
[27] A. Thawko, A. Eyal, L. Tartakovsky, Experimental comparison of performance and emissions of a direct-injection engine fed with alternative gaseous fuels, Energy Convers. Manag. 251 (2022) 114988, https://doi.org/10.1016/j.enconman.2021.114988.
[28] A. Thawko, H. Yadav, A. Eyal, M. Shapiro, L. Tartakovsky, Particle emissions of direct injection internal combustion engine fed with a hydrogen-rich reformate, Int. J. Hydrog. Energy 44 (2019) 28342–28356, https://doi.org/10.1016/j.ijhydene.2019.09.062.
[29] A. Thawko, L. Tartakovsky, The mechanism of particle formation in non-premixed hydrogen combustion in a direct-injection internal combustion engine, Fuel 327 (2022) 125187, https://doi.org/10.1016/j.fuel.2022.125187.
[30] B. Apicella, F. Catapano, S. Di Iorio, A. Magno, C. Russo, P. Sementa, et al., Comprehensive analysis on the effect of lube oil on particle emissions through gas exhaust measurement and chemical characterization of condensed exhaust from a DI SI engine fueled with hydrogen, Int. J. Hydrog. Energy 48 (2023) 22277–22287, https://doi.org/10.1016/j.ijhydene.2023.03.112.
[31] B. Apicella, F. Catapano, S. Di Iorio, A. Magno, C. Russo, P. Sementa, et al., Comprehensive analysis on the effect of lube oil on particle emissions through gas exhaust measurement and chemical characterization of condensed exhaust from a DI SI engine fueled with hydrogen. Part 2: Effect of operating conditions, Int. J. Hydrog. Energy 49 (2024) 968–979, https://doi.org/10.1016/j.ijhydene.2023.09.279.
[32] S. Di Iorio, P. Sementa, B.M. Vaglieco, F. Catapano, An experimental investigation on combustion and engine performance and emissions of a methane-gasoline dual-fuel optical engine, SAE Tech Pap, 2014, p. 1, https://doi.org/10.4271/2014-01-1329.
[33] TSI Incorporated, Engine Exhaust Particle Sizer ™ Spectrometer Model 3090 March 2015, 2015. https://tsi.com/products/particle-sizers/fast-particle-sizer-spectrometers/engine-exhaust-particle-sizer-(eeps)-3090/.
[34] C. Russo, A. Carpentieri, A. Tregrossi, A. Ciajolo, B. Apicella, Blue, green and yellow carbon dots derived from pyrogenic carbon: structure and fluorescence behaviour, Carbon N Y 201 (2023) 900–909, https://doi.org/10.1016/j.carbon.2022.09.062.
[35] C. Russo, A. Ciajolo, F. Stanzione, A. Tregrossi, B. Apicella, Separation and online optical characterization of fluorescent components of pyrogenic carbons for carbon dots identification, Carbon N Y 209 (2023) 118009, https://doi.org/10.1016/j.carbon.2023.118009.
[36] E. Yilmaz, T. Tian, V.W. Wong, J.B. Heywood, The Contribution of different oil consumption sources to total oil consumption in a spark ignition engine, SAE Tec Pap, 2004, 2004-01-2909.
[37] R. Amirante, E. Distaso, M. Napolitano, P. Tamburrano, Iorio S. Di, P. Sementa, et al., Effects of lubricant oil on particulate emissions from port-fuel and direct-injection spark-ignition engines, Int. J. Engine Res. 18 (2017) 606–620, https://doi.org/10.1177/1468087417706602.
[38] I.B. Berlman, Fluorescence Spectra of Aromatic Molecules, Academic Press, New York and London, 1971.
[39] T. Vo-Dinh, Multicomponent analysis by synchronous luminescence spectrometry, Anal. Chem. 50 (1978) 396–401, https://doi.org/10.1021/ac50025a010.
[40] B. Apicella, A. Ciajolo, A. Tregrossi, Fluorescence spectroscopy of complex aromatic mixtures, Anal. Chem. 76 (2004) 2138–2143, https://doi.org/10.1021/ac034860k.
[41] F. Catapano, S. Di Iorio, A. Magno, P. Sementa, B.M. Vaglieco, A comparison of methanol, methane and hydrogen fuels for si engines: Performance and pollutant emissions, SAE Tec Pap, 2023, p. 9, https://doi.org/10.4271/2023-24-0037. Received, 2023-24-0037.
[42] F. Catapano, Iorio S. Di, A. Magno, P. Sementa, B.M. Vaglieco, A complete assessment of the emission performance of an si engine fueled with methanol, methane hydrogen, Energies 17 (2024) 1026.
[43] F. Catapano, S. Di Iorio, A. Magno, P. Sementa, B.M. Vaglieco, A comprehensive analysis of the effect of ethanol, methane and methane-hydrogen blend on the combustion process in a PFI (port fuel injection) engine, Energy 88 (2015) 101–110, https://doi.org/10.1016/j.energy.2015.02.051.
[44] A.P. Singh, A. Pal, N.K. Gupta, A.K. Agarwal, Particulate emissions from laser ignited and spark ignited hydrogen fueled engines, Int. J. Hydrog. Energy 42 (2017) 15956–15965, https://doi.org/10.1016/j.ijhydene.2017.04.031.
[45] D.R. Tree, K.I. Svensson, Soot processes in compression ignition engines, Prog. Energy Combust. Sci. 33 (2007) 272–309, https://doi.org/10.1016/j.pecs.2006.03.002.